quired to antibody carriers, and result in a reduction of side effects.

As next step, we are trying to evaluate its antibody evasion ability *in vivo* aiming for clinical use. Especially considering that the PEG-Ad used in this study was with low modification rate (34%, confirmed by SDS-PAGE, Fig. 2), we anticipated that highly modified PEG-Ad would protect it from neutralizing antibody more efficiently *via* stronger steric hindrance of PEG chains. Including of the other merits possessed by PEG-Ad, such as the extension of blood retention half-time and reduction of antigenicity. These approaches which are applicable to other vectors and other high compounds will promote development of the novel intelligent virus vectors.

Acknowledgements This study was supported in part by the Research on Health Sciences focusing on Drug Innovation from The Japan Health Sciences Foundation; by Grants-in-Aid for Exploratory Research from the Ministry of Education, Culture, Sports, Science and Technology of Japan; and by grants from the Ministry of Health and Welfare in Japan.

Y. Eto and J. Gao contributed equally to the work.

REFERENCES

1) Gao J. Q., Tsuda Y., Katayama K., Nakayama T., Hatanaka Y., Tani Y., Mizuguchi H., Hayakawa T., Yoshie O., Tsutsumi Y., Mayumi T., Nakagawa S., *Cancer Res.*, **63**, 4420—4425 (2003).
2) Crystal, R. G., *Science*, **270**, 404—410 (1995).
3) Wilson J. M., *N. Engl. J. Med.*, **334**, 1185—1187 (1996).
4) Smith T. A., Mchaffey M. G., Kayda D. B., Saunders J. M., Yei S., Trapnell B. C., McClelland A., Kaleko M., *Nat. Genet.*, **5**, 397—402 (1993).
5) Hitt M., Addison C., Graham F., *Adv. Pharmacol.*, **40**, 137—206 (1997).
6) Connelly S., Andrews J. L., Gallo A. M., Kayda D. B., Qian J., Hoyer L., Kadan M. J., Gorziglia M. I., Trapnell B. C., McClelland A., Kaleko M., *Blood*, **91**, 3273—3281 (1998).
7) Zimmer K. P., Bendiks M., Mori M., Kominami E., Robinson M. B., Ye X., Wilson J. M., *Mol. Med.*, **5**, 244—253 (1999).
8) Wohlfart C., *J. Virol.*, **62**, 2321—2328 (1988).
9) Mastrangeli A., Harvey B. G., Yao J., Wolff G., Kovesdi I., Crystal R. G., Falck-Pedersen E., *Hum. Gene Ther.*, **7**, 79—87 (1996).
10) Yei S., Mittereder N., Tang K., O'Sullivan C., Trapnell B. C., *Gene Ther.*, **1**, 192—200 (1994).
11) Inada Y., Furukawa M., Sasaki H., Kodera Y., Hiroto M., Nishimura H., Matsushima A., *Trends Biotechnol.*, **13**, 86—91 (1995).
12) Tsutsumi Y., Tsunoda S., Kamada H., Kihira T., Nakagawa S., Kaneda Y., Kanamori T., Mayumi T., *Br. J. Cancer*, **74**, 1090—1095 (1996).
13) Von Seggern D. J., Chiu C. Y., Fleck S. K., Stewart P. L., Nemerow G. R., *J. Virol.*, **73**, 1601—1608 (1999).
14) Koizumi N., Mizuguchi H., Sakurai F., Yamaguchi T., Watanabe Y., Hayakawa T., *J. Virol.*, **77**, 13062—13072 (2003).
15) Mizuguchi H., Kay M. A., *Hum. Gene Ther.*, **9**, 2577—2583 (1998).
16) Maizel J. V., Jr., White D. O., Scharff M. D., *Virology*, **36**, 115—125 (1968).
17) Li W. M., Mayer L. D., Bally M. B., *J. Pharmacol. Exp. Ther.*, **300**, 976—983 (2002).
18) Chillon M., Lee J. H., Fasbender A., Welsh M. J., *Gene Ther.*, **5**, 995—1002 (1998).
19) Tsutsumi Y., Kihira T., Tsunoda S., Kamada H., Nakagawa S., Kaneda Y., Kanamori T., Mayumi T., *J. Pharmacol. Exp. Ther.*, **278**, 1006—1011 (1996).

Department of Biopharmaceutics[1], Graduate School of Pharmaceutical Sciences, Osaka University, Japan, Department of Pharmaceutics[2], School of Pharmaceutical Sciences, Zhejiang University, P.R. China, Division of Cellular and Gene Therapy Products[3], National Institute of Health Sciences, Japan, Department of Microbiology[4], Kinki University School of Medicine, Japan

Tumor-suppressive activities by chemokines introduced into OV-HM cells using fiber-mutant adenovirus vectors

J.Q. GAO[1,2], L.S. ALEXANDRE[1], Y. TSUDA[1], K. KATAYAMA[1], Y. ETO[1], F. SEKIGUCHI[1], H. MIZUGUCHI[3], T. HAYAKAWA[3], T. NAKAYAMA[4], O. YOSHIE[4], Y. TSUTSUMI[1], T. MAYUMI[1], S. NAKAGAWA[1]

Received September 11, 2003, accepted September 19, 2003

Shinsaku Nakagawa, Ph.D., Department of Biopharmaceutics, Graduate School of Pharmaceutical Sciences, Osaka University, Yamadaoka 1–6, 565-0871 Suita City, Osaka, Japan
nakagawa@phs.osaka-u.ac.jp

Pharmazie 59: 238–239 (2004)

In this study, fiber-mutant adenovirus vectors encoding chemokines, Ad-RGD-mCCL17, Ad-RGD-mCCL21 and Ad-RGD-mCCL22 were constructed. The insertion of integrin-targeting RGD sequence into fiber knob of adenovirus vectors notably enhanced the infection efficiency into tumor cells. Among three chemokine-encoding vectors evaluated, Ad-RGD-mCCL22 showed significant tumor-suppressive activity via transduction into OV-HM cells.

Cytokine or chemokine encoded by a viral vector is currently regarded as a promising way of cancer gene immunotherapy. Chemokines consist of a superfamily of small secreted proteins that attract their target cells by interacting with G protein-coupled receptors expressed on these cells. Researchers have paid attention to chemotactic activity of chemokines for immune cells, and have expected that they may be able to play a pivotal role in cancer treatment, because the basis and premise of immunotherapy is the accumulation of immune cells in tumor tissues. More than 40 chemokines have been identified so far (Yoshie et al. 2001), but only a few have been demonstrated as candidates for cancer therapy by using as sole agents or with adjuvant (Gao et al. 2003; Maric and Liu 1999).

In the present report, three CC family chemokines, thymus and activation-regulated chemokine/CCL17, secondary lymphoid-tissue chemokine/CCL21 and macrophage-derived chemokine/CCL22 have been studied. CCL17 and CCL22 are chemotactic for memory CD4 + T cells via CCR4 while CCL21 induces migration of T cells, B cells, dendritic cells and NK cells via CCR7 (Campbell et al. 1999, Nagira et al. 1997). CCL22 was also shown to have a chemoattractant activity for dendritic cells, NK cells and T cells (Godiska et al. 1997). We hypothesized that if tumor cells could be genetically modified *in vitro* to produce chemokines *in vivo*, the chemokines would accumulate immune cells in the tumor. The facilitated interaction of immune cells with the tumor cells *in vivo* might induce anti-tumor activity. To test this hypothesis, we developed a recombinant adenovirus vector with a fiber mutation containing the integrin-targeting Arg-Gly-Asp (RGD) sequence in the fiber knob (Mizuguchi et al. 2001b). As shown in the Table, This vector has been demonstrated to possess higher transduction efficacy to OV-HM cells, a mouse ovary carcinoma line (Hashimoto et al. 1989), compared to that of conventional adenovirus vector.

Table: EGFP expression in OV-HM cells infected with Ad-EGFP and Ad-RGD-EGFP

	250 PT % gated	500 PT % gated
Non-infection	0.94%	0.94%
Ad-EGFP	47.1%	76.3%
Ad-RGD-EGFP	98.7%	99.6%

OV-HM cells were infected with 250 or 500 particles/cell of Ad-EGFP or Ad-RGD-EGFP for 48 h and EGFP expression was measured by flow cytometric analysis

In this study, we infected OV-HM with fiber-mutant adenovirus vectors encoding mCCL17, mCCL21 or mCCL22 and examined their expression by RT-PCR. The migration assay of chemokine-encoding vectors was also conducted *in vitro*. The results demonstrated that the efficient production of biologically active mCCL17, mCCL21 and mCCL22 could be detected in the culture supernatants of cells infected with these vectors, and the vectors could efficiently migrate the specific receptor-expressing cells (data not shown). Then OV-HM cells infected with Ad-RGD-mCCL17, Ad-RGD-mCCL21, Ad-RGD-mCCL22 or Ad-RGD-NULL (the control vector only) were intradermally inoculated into B6C3F1 mice to evaluate their effects on tumor growth *in vivo*. As shown in the Fig., OV-HM infected with Ad-RGD-mCCL22 showed significant suppression in tumor growth. On the other hand, OV-HM infected with either Ad-RGD-mCCL17 or Ad-RGD-mCCL21 did not show any difference in tumor growth from that infected with Ad-RGD-NULL. In rechallenge experiment, mice that had complete regression were intradermally injected with OV-HM or B16/BL6 cells 90 days after the initial challenge. Results demonstrated that 100% of mice rechallenged with OV-HM remained tumor-free. In contrast, all of the mice rechallenged with B16/BL6 developed palpable tumors within 2 weeks (data not shown). These results indicated the generation of specific immunity against OV-HM in mice that rejected OV-HM expressing mCCL22. To exclude the possibility that the growth suppression of the tumor cells by Ad-RGD-mCCL22 was due to the cytotoxicity of adenovirus or

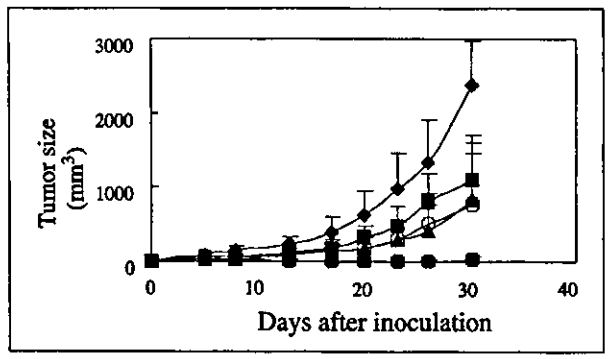

Fig.: Tumor-suppressive activity of Ad-RGD-mCCL22
—◆— No-treat, —■—Ad-RGD-NULL, —▲— Ad-RGD-mCCL17, —●— Ad-RGD-mCCL22, —○— Ad-RGD-mCCL21

chemokine, OV-HM cells transfected with Ad-RGD-mCCL17, Ad-RGD-mCCL21, Ad-RGD-mCCL22 or Ad-RGD-NULL were cultured for 48 h, and the cell viability was measured by the MTT assay. The *in vitro* growth of the cells infected with these vectors was essentially identical to that of control cells (data not shown).

In summary, our study suggests that CCL22, a CC family chemokine, may be a good candidate for cancer gene immunotherapy.

Experimental

1. Cell lines and animals

OV-HM ovarian carcinoma cells were kindly provided by Dr. Hiromi Fujiwara (School of Medicine, Osaka University, Japan) and were maintained in RPMI 1640 supplemented with 10% heat-inactivated FBS. Human embryonic kidney (HEK) 293 cells were cultured in DMEM supplemented with 10% FBS. All the cell lines were cultured at 37 °C in a humidified atmosphere with 5% CO_2. Female B6C3F1 mice (6–8 week of age) were purchased from SLC Inc. (Hamamatsu, Japan). All of the experimental procedures were in accordance with the Osaka University guidelines for the welfare of animals in experimental neoplasia.

2. Procedures

2.1. Infection of chemokines into OV-HM cells using fiber-mutant adenovirus vectors

Replication-deficient adenovirus vectors used in this study were based on the adenovirus serotype 5 backbone with deletions of E1 and E3 and the expression cassette in the E1 region (Mizuguchi et al. 2001a). The integrin-targeting RGD sequence was inserted into the HI loop of the fiber knob using a two-step method (Mizuguchi et al. 2001b). Fiber-mutant adenovirus vectors, Ad-RGD-mCCL17, Ad-RGD-mCCL21 and Ad-RGD-mCCL22 carrying the murine chemokine cDNA under the control of the cytomegalovirus promoter, were constructed by an improved *in vitro* ligation method as described (Mizuguchi and Kay 1998). The Ad-RGD-NULL vector, serving as a negative control, is identical to the Ad-RGD-chemokine vectors without the chemokine gene in the expression cassette. The adenovirus vectors were propagated in HEK 293 cells and purified by cesium chloride gradient ultracentrifugation, and their titer was determined by plaque-forming assay.

2.2. Tumor rejection in mice and subsequent rechallenge by tumor reinoculation

1×10^6 OV-HM cells that had been infected with Ad-RGD-mCCL17, Ad-RGD-mCCL21 or Ad-RGD-mCCL22 at a MOI (Multiplicity of Infection) of 10 for 24 h were inoculated intradermally into the flank of mice. The length and width of the tumor were measured twice a week. Animals were euthanized when one of the two measurements were greater than 15 mm. Three months after complete regression of primary tumors, mice were rechallenged with freshly isolated OV-HM tumor cells or B16/BL6 melanoma cells by intradermal injection of 1×10^6 cells into the flank.

References

Campbell JJ, Haraldsen G, Pan J et al. (1999) The chemokine receptor CCR4 in vascular recognition by cutaneous but not intestinal memory T cells. Nature 400: 776–780.

Gao JQ, Tsuda Y, Katayama K et al. (2003) Anti-tumor effect by interleukin-11 receptor alpha-locus chemokine/CCL27, introduced into tumor cells through a recombinant adenovirus vector. Cancer Res 63: 4420–4425.

Godiska R, Chantry D, Raport CJ et al. (1997) Human macrophage-derived chemokine (MDC), a novel chemoattractant for monocytes, monocyte-derived dendritic cells, and natural killer cells. J Exp Med 185: 1595–1604.

Hashimoto M, Niwa O, Nitta Y et al. (1989) Unstable expression of E-Cadherin adhesion molecules in metastatic ovarian tumor cells. Jpn J Cancer Res 80: 459–463.

Maric M, Liu Y (1999) Strong cytotoxic T lymphocyte responses to a macrophage inflammatory protein 1 alpha-expressing tumor: linkage between inflammation and specific immunity. Cancer Res 59: 5549–5553.

Mizuguchi H, Kay MA, Hayakawa T (2001a) In vitro ligation-based cloning of foreign DNAs into the E3 and E1 deletion regions for generation of recombinant adenovirus vectors. Biotechniques 30: 1112–1114.

Mizuguchi H, Koizumi N, Hosono T et al. (2001b) A simplified system for constructing recombinant adenoviral vectors containing heterologous peptides in the HI loop of their fiber knob. Gene Ther 8: 730–735.

Mizuguchi H, Kay MA (1998) Efficient construction of a recombinant adenovirus vector by an improved *in vitro* ligation method. Hum Gene Ther 9: 2577–2583.

Nagira M, Imai T, Hieshima K et al. (1997) Molecular cloning of a novel human CC chemokine secondary lymphoid-tissue chemokine that is a potent chemoattractant for lymphocytes and mapped to chromosome 9p 13. J Biol Chem 272: 19518–19524.

Yoshie O, Imai T, Nomiyama H (2001) Chemokines in immunity. Adv Immunol 78: 57–110.

Available online at www.sciencedirect.com
SCIENCE DIRECT®
Biomaterials 25 (2004) 4309–4315
Biomaterials
www.elsevier.com/locate/biomaterials

The targeting of anionized polyvinylpyrrolidone to the renal system

Hiroshi Kodaira[1], Yasuo Tsutsumi*,[1], Yasuo Yoshioka[1], Haruhiko Kamada, Yoshihisa Kaneda, Yoko Yamamoto, Shin-ichi Tsunoda, Takayuki Okamoto, Yohei Mukai, Hiroko Shibata, Shinsaku Nakagawa, Tadanori Mayumi

Graduate School of Pharmaceutical Sciences, Department of Biopharmaceutics, Osaka University, 1-6 Yamadaoka, Suita, Osaka 565-0871, Japan

Received 5 October 2003; accepted 24 October 2003

Abstract

We reported that the co-polymer composed of vinylpyrrolidone and maleic acid selectively distributed into the kidneys after i.v. injection. To further optimize the renal drug delivery system, we assessed the renal targeting capability of anionized polyvinylpyrrolidone (PVP) derivatives after intravenous administration in mice. The elimination of anionized PVP derivatives from the blood decreased with increasing anionic groups, and the clearance of carboxylated PVP and sulfonated PVP from the blood was almost similar. But carboxylated PVP efficiently accumulated in the kidney, whereas sulfonated PVP was rapidly excreted in the urine. The renal levels of carboxylated PVP were about five-fold higher than sulfonated PVP. Additionally, carboxylated PVP was effectively taken up by the renal proximal tubular epithelial cells in vivo after i.v. injection. These anionized PVP derivatives did not show any cytotoxicity against renal tubular cells and endothelial cells in vitro. Thus, these carboxylated and sulfonated PVPs may be useful polymeric carriers for drug delivery to the kidney and bladder, respectively.

Keywords: Polyvinylpyrrolidone (PVP); Renal targeting; Drug carrier; Bioconjugation

1. Introduction

Renal disease is a serious health problem which is on the increase in the world [1,2]. They face a future on dialysis and may require a kidney transplant. While dialysis and renal transplantation are life-saving, they are expensive and do not restore normal health. Therefore, new therapeutic strategies must be developed for treating patients with renal disease. Drugs such as steroids have been used to prevent the progression of renal disease, but they produced toxicity because of their wide distribution in the body. The development of a renal delivery system that selectively carries drugs to the kidneys is a promising approach for limiting tissue distribution and controlling toxicity. While many drug carriers are available for the liver and tumor, few effective carriers are available for the kidneys.

Recently, we synthesized polyvinylpyrrolidone-co-dimethyl maleic anhydride [poly(VP-co-DMMAn)] as a novel polymeric drug carrier for a renal drug delivery system [3]. Our results showed that when poly(VP-co-DMMAn) was conjugated with amino groups of drugs, these conjugates showed much higher accumulation and retention in the kidneys without any adverse toxicity. Additionally, poly(VP-co-DMMAn) was specifically taken up by the renal proximal tubular epithelial cells in vivo, and poly(VP-co-DMMAn)-modified anti-inflammatory proteins accelerated recovery from acute renal failure. These results strongly indicated that anionized polyvinylpyrrolidone (PVP) derivatives may be powerful candidates as renal targeting carriers.

In this study, we have focused on the assessment of the in vivo behavior of anionized PVP derivatives for optimizing the renal drug delivery system. To evaluate the relationship between pharmacokinetics and their anionic functional groups, copolymers of carboxylated PVP [poly(vinylpyrrolidone-co-acrylic acid)] and sulfonated PVP [poly(vinylpyrrolidone-co-vinylsulfonic acid)] were synthesized by radical polymerization. This study may provide useful information, which will

*Corresponding author. Tel.: +81-66879-8178; fax: +81-66879-8178.
E-mail address: tsutsumi@phs.osaka-u.ac.jp (Y. Tsutsumi).
[1]These authors contributed equally to the work.

0142-9612/$ - see front matter © 2003 Elsevier Ltd. All rights reserved.
doi:10.1016/j.biomaterials.2003.10.097

facilitate the optimal molecular design of polymeric drug carriers applicable to the therapeutic use of the drug delivery system for the urinary organ.

2. Materials and methods

2.1. Materials

Chemicals were purchased from Wako Pure Chemical Industries Ltd. (Osaka, Japan). TSKgel G4000PW and TSKgel alpha-3000 columns were obtained from Tosoh Corporation (Tokyo, Japan). $Na^{125}I$ (3.7 GBq/ml) solution was obtained from NEN Research Products (Boston, MA, USA).

2.2. Animals and cells

All the experimental protocols for the animal studies were in accordance with the "Guide for laboratory Animal Facilities and Care" (NIH publication 85–23, revised 1985). These protocols have been approved by the committee in Pharmaceutical School, Osaka University. Male ddY mice were obtained from SLC (Hamamatsu, Japan). Sarcoma-180 cells (S-180, Cancer Cell Repository Institute of Development, Aging and Cancer, Tohoku University) were maintained intraperitoneally by serial passages in ddY mice. Normal human aortic endothelial cells and mouse renal tubular (LLC-MK2) cells were cultured in HuMedia-EG2 or MEM supplemented with 10% fetal bovine serum, respectively.

2.3. Synthesis of PVP and its anionized derivatives

PVP was synthesized by the radical polymerization method using 4,4′-azobis-4-cyanovaleric acid (ACVA) and β-mercaptopropionic acid (β-MP) as the radical initiator and chain transfer agent, respectively. The anionized PVP derivatives of both carboxylated PVP [poly(vinylpyrrolidone-co-acrylic acid)] and sulfonated PVP [poly(vinylpyrrolidone-co-vinylsulfonic acid)] were prepared by radical co-polymerization of VP and anionic co-monomers (acrylic acid or vinylsulfonic acid) in DMF with the aid of ACVA and MPA. The molar ratio of VP and anionic co-monomers was 19:1 for 5%-anionized PVP (5%-carboxylated PVP and 5%-sulfonated PVP) or 4:1 for 20%-anionized PVP (20%-carboxylated PVP and 20%-sulfonated PVP). These polymers were separated into several fractions by GFC to obtain polymers with a narrow molecular weight distribution. The number-average molecular weight of PVP and both the anionized PVP derivatives was about 10 kDa (polydispersity $[M_w/M_n] < 1.39$; PEG standards). The co-monomer content determined by ^{1}H-NMR was in good agreement with the feed molar ratio of anionic co-monomer relative to VP monomer.

2.4. In vivo behavior of polymers

^{125}I-radiolabeled polymers were prepared by the chloramine-T method, and purified by GFC. The specific activities of ^{125}I-labeled polymers were about 4.44 μCi/mg polymer. S-180 cells were implanted intradermally (5×10^5 cells/200 μl/site) in mice that were injected i.v. with ^{125}I-labeled polymer (1×10^6 cpm/200 μl) seven days later when the diameter of the tumors exceeded 7 mm. Blood was collected from the tail vein at intervals and the radioactivity was measured. GFC analysis confirmed that more than 95% of the radioactivity in circulating blood 3 h after i.v. injection was derived from intact ^{125}I-labeled polymers. Mice were housed in metabolic cages for urine collection and were killed 3 h after the treatment to evaluate tissue distribution.

2.5. Histological analysis of renal tissues

Mice were i.v. injected with amino-aceto-fluorescein (AAF)-labeled polymers, and the kidneys were collected 3 h later. Under ether anesthesia, the kidneys were excised and immersed in liquid nitrogen. Histological sections were prepared by microtome, mounted on silane-coated glass slides, and observed under fluorescent microscopy.

2.6. In vitro cytotoxicity of polymers

The cytotoxicity of PVP and anionized PVP derivatives were measured in LLC-MK2 and HAEC cells. The cells were seeded in 96-well plates at a concentration of 4.0×10^4 cells/100 μl per well. After a 12 h incubation, each polymer was added in a volume of 100 μl at threefold dilution. The plates were incubated for 19 h at 37°C, and the viability of the cells was determined by MTT assay. All polymer dilutions were tested in triplicate.

3. Results

3.1. Plasma clearance

The anionized PVP derivatives were separated and purified by GFC to adjust the molecular size (10 kDa) and the polydispersity of PVP. The plasma clearance of PVP and anionized PVP derivatives were compared in mice bearing S-180 solid tumors (Fig. 1). Both the carboxylated and sulfonated PVP were cleared more quickly from the blood than PVP after i.v. injection. The clearance of carboxylated PVP from blood was similar to sulfonated PVP. The elimination of anionized PVPs decreased as the number of anionic groups increased. The mean residence times (MRT) of PVP 5%-,

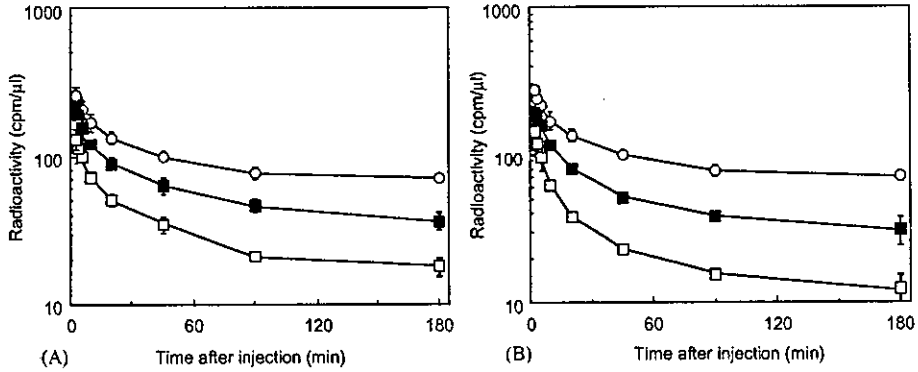

Fig. 1. Plasma clearance of PVP and anionized PVP derivatives after i.v. injection in mice. Mice were intravenously injected with ^{125}I-labeled PVPs. After administration, blood was collected from the tail at indicated times and the radioactivity was measured by a γ-counter. Mice were used in groups of five. Each value is the mean±S.D. (A) PVP (○), 5%-carboxylated PVP (■), 20%-carboxylated PVP (□). B: PVP (○), 5%-sulfonated PVP (■), 20%-sulfonated PVP (□).

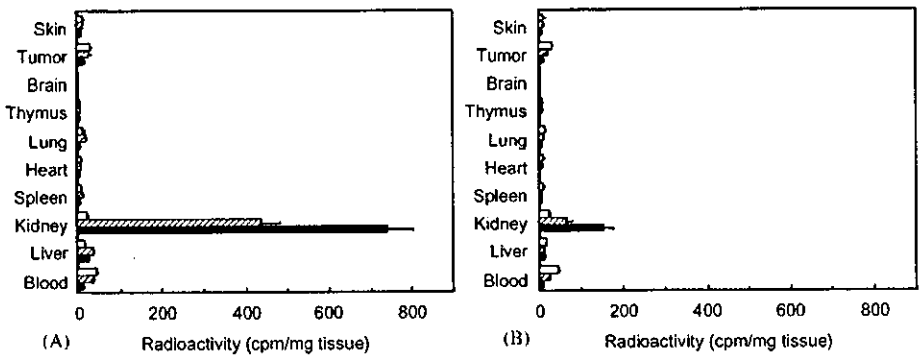

Fig. 2. Tissue distribution of PVP and anionized PVP derivatives at 3 h after i.v. injection in mice. Mice were intravenously injected with ^{125}I-labeled polymers. After i.v. injection, mice were killed and the organs were collected. The radioactivity was measured by a γ-counter. Mice were used in groups of five. Each value is the mean±S.D. (A) PVP (□), 5%-carboxylated PVP (▨), 20%-carboxylated PVP (■) (B) PVP (□), 5%-sulfonated PVP (▨), 20%-sulfonated PVP (■).

20%-carboxylated PVP, 5%-, 20%-sulfonated PVP were 302.4±62.5 and 196.7±58.9 min, 174.3±56.3, 200.1±34.7, and 176.0±61.3 min, respectively.

3.2. Tissue distribution

The tissue distributions of PVP and anionized PVP derivatives that had the same molecular size were measured 3 h after i.v. injection (Fig. 2). No significant radioactivity was observed in the thyroid gland for any of the polymers. Since free ^{125}I molecules rapidly accumulate in the thyroid gland, this indicates that negligible free ^{125}I was released from the labeled polymers during the study, and shows that ^{125}I-labeled polymers were stable in the body during the distribution experiment. In fact, gel filtration chromatography analysis confirmed that the almost all of the radioactivity in circulating blood 3 h after i.v. injection were derived from intact ^{125}I-labeled polymers. PVP showed little tissue-specific localization. The anionized PVP derivatives, on the other hand, effectively accumulated in the kidney, as compared with other tissues. Especially, the carboxylated PVPs showed higher renal accumulation than the sulfonated PVPs, and about 30% of the administered dose of 20%-carboxylated PVP was observed in the kidney. An increase in the content of carboxyl groups in the PVP increased the renal radioactivity. But, polyacrylic acid (PAA; 100%-carboxylated homopolymer) showed little accumulation in the kidney (data not shown). These results suggested that carboxylated PVP with optimal anionic groups may produce the highest renal levels. Mice were i.v. injected with fluorescent labeled-polymers (PVP and 20%-carboxylated PVP, 20%-sulfonated PVP) and their kidneys were collected after 3 h. The sections were prepared and evaluated by fluorescent microscopy (Fig. 3). Most of the 20%-carboxylated PVP accumulated in the renal tubules, especially the proximal tubular epithelial cells, but not in glomeruli, whereas PVP did not accumulate in the renal tubules. In

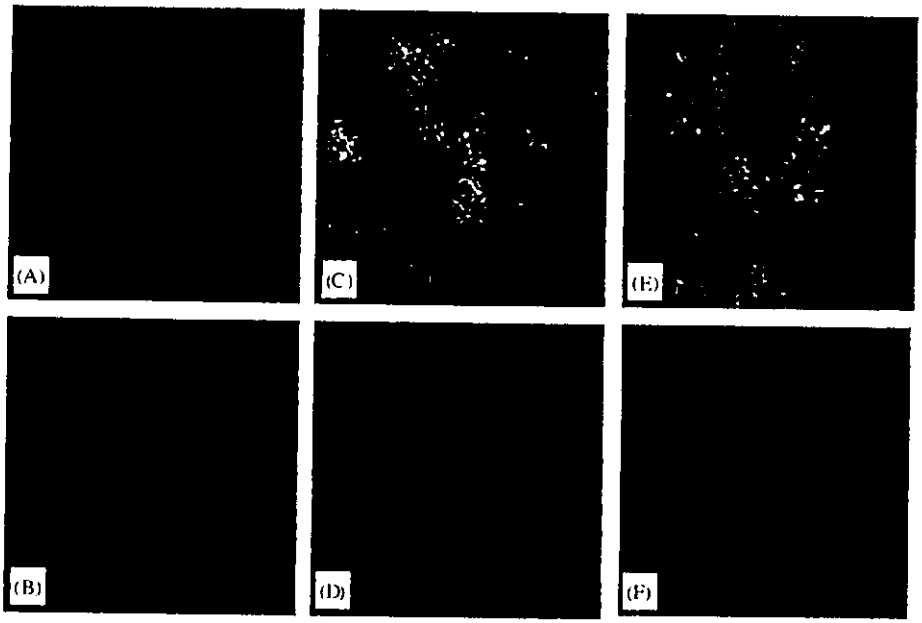

Fig. 3. Histological sections of renal tissues in mice receiving injection of fluorescein-labeled anionized PVPs. BALB/c mice were injected intravenously with (A); aminoacetofluorescein (AAF)-conjugated PVP, (B); AAF, (C); AAF-conjugated carboxylated PVP, (D); mixture between AAF and carboxylated PVP (no conjugation), (E); AAF-conjugated sulfonated PVP, (F); mixture between AAF and sulfonatated PVP (no conjugation).

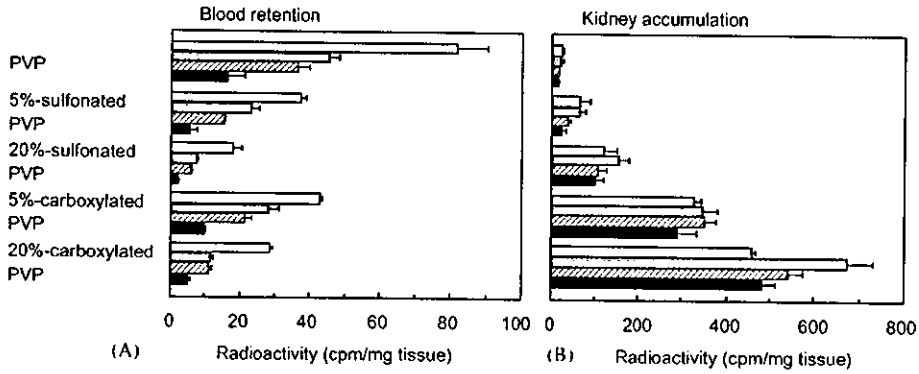

Fig. 4. Blood retention and kidney accumulation of PVP and anionized PVP derivatives after i.v. injection in mice. Mice were intravenously injected with ^{125}I-labeled polymers. At the indicated times after i.v. injection of PVP and anionized PVP derivatives, mice were sacrificed, and blood (A) and kidneys (B) were collected. The radioactivity was measured using a γ-counter. Mice were used in groups of five. Each value is the mean±S.D. were used in groups of five. Each value is the mean±S.D. (□): 1 h, (■): 3 h, (□): 6 h, (■): 24 h after i.v. injection.

contrast, 20%-sulfonated PVP slightly existed in the kidneys. Neither AAF nor the mixture between polymer and AAF were detected in the renal tubules.

3.3. Renal levels after i.v. injection

The blood levels of all polymers decreased rapidly 24 h after i.v. injection (Fig. 4). PVP did not accumulate in the kidneys, while anionized PVP derivatives accumulated in the kidneys over the period studied. The maximal renal levels occurred 3 h after treatment and slowly declined over time. Especially, 20%-carboxylated PVP was thirty-two times higher than PVP 24 h after i.v. injection. These results suggested that carboxylated PVP rapidly distributed into the kidney and was gradually excreted into the urine, whereas sulfonated PVPs were quickly excreted into the urine. In contrast, PVP was effectively retained in the blood and gradually excreted into the urine without concentrating in the kidneys.

3.4. Cytotoxicity

The biocompatibility of PVP and anionized PVP derivatives were compared to polybrene, a cytotoxic

[2] Progress and Priorities: Renal disease research plan. Report of the strategic planning conferences—Renal research properties—sponsored by National Institute of Diabetes and Digestive and Kidney Disease. Council of American Kidney Socities (December 5–6, 1998 & February 4–5, 1999). (http://www.niddk.nih.gov/federal/planning.htm#g).

[3] Kamada H, Tsutsumi Y, Sato-Kamada K, Yamamoto Y, Yoshioka Y, Okamoto T, Nakagawa S, Nagata S, Mayumi T. Synthesis of a poly(vinylpyrrolidone-co-dimethyl maleic anhydride) co-polymer and its application as renal targeting carrier. Natl Biotechnol 2003;21:399–404.

[4] Yamamoto Y, Tsutsumi Y, Yoshioka Y, Nishibata T, Kobayashi K, Okamoto T, Mukai Y, Shimizu T, Nakagawa S, Nagata S, Mayumi T. Site-specific PEGylation of a lysine-deficient TNF-alpha with full bioactivity. Nat. Biotechnol 2003;21:546–52.

[5] Tsutsumi Y, Onda M, Nagata S, Lee B, Kreitman RJ, Pastan I. Site-specific chemical modification with polyethylene glycol of recombinant immunotoxin anti-Tac(Fv)-PE38 (LMB-2) improves antitumor activity and reduces animal toxicity and immunogenicity. Proc Natl Acad Sci USA 2000;97:8548–53.

[6] Kamada H, Tsutsumi Y, Yamamoto Y, Kihira T, Kaneda Y, Mu Y, Kodaira H, Tsunoda S, Nakagawa S, Mayumi T. Antitumor activity of tumor necrosis factor-alpha conjugated with polyvinylpyrrolidone on solid tumors in mice. Cancer Res 2000;60:6416–20.

[7] Kaneda Y, Yamamoto Y, Kamada H, Tsunoda S, Tsutsumi Y, Hirano T, Mayumi T. Antitumor activity of tumor necrosis factor-alpha conjugated with diviny ether and maleic anhydride copolymer on solid tumors in mice. Cancer Res 1998;58:290–5.

[8] Inoue M, Ebashi I, Watanabe N, Morino Y. Synthesis of a superoxide dismutase derivative that circulates bound to albumin and accumulates in tissues whose pH is decreased. Biochemistry 1989;28:6619–24.

[9] Simionescu N. Cellular aspects of transcapillary exchange. Physiol Rev 1983;63:1536–79.

[10] Chang RL, Deen WM, Robertson CR, Brenner BM. Permselectivity of the glomerular capillary wall: III. Restricted transport of polyanions. Kidney Int 1975;8:212–8.

[11] Takakura Y, Fujita T, Hashida M, Sezaki H. Disposition characteristics of macromolecules in tumor-bearing mice. Pharm Res 1990;7:339–46.

[12] Elfarra AA, Duescher RJ, Hwang IY, Sicuri AR, Nelson JA. Targeting 6thioguanine to the kidney with S-(guanin-6-yl)-L-cysteine. J Pharmacol Exp Ther 1995;274:1298–304.

[13] Haverdings RF, Haas M, Greupink AR, de Vries PA, Moolenaar F, de Zeeuw D, Meijer DK. Potentials and limitations of the low-molecular-weight protein lysozyme as a carrier for renal drug targeting. Ren Fail 2001;23:397–409.

[14] Schechter B, Arnon R, Colas C, Burakova T, Wilchek M. Renal accumulation of streptavidin: potential use for targeted therapy to the kidney. Kidney Int 1995;47:1327–35.

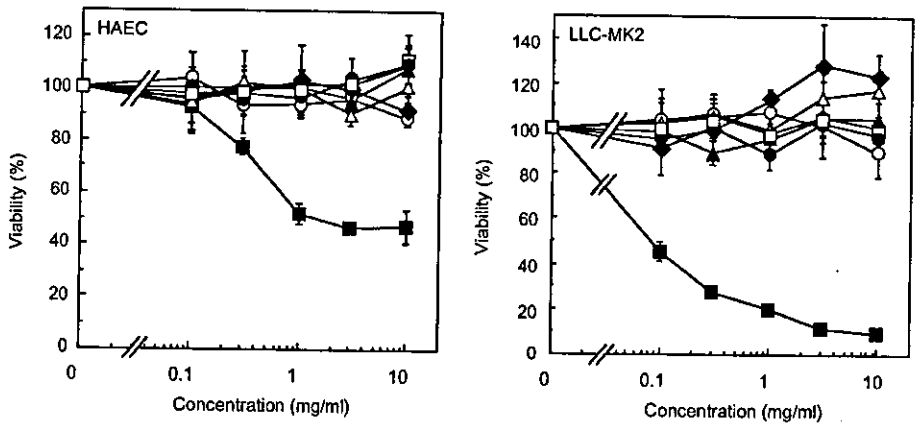

Fig. 5. Cytotoxicity of various polymers to HAEC and LLC-MK2 evaluated by MTT assay. The cells of HAEC and LLC-MK2 were incubated for 24 h with PVP, anionized PVP derivatives and polybrene (positive control) at five different concentrations in each medium. The cell viabilities were determined using a microplate reader after dying with formazan. Each value is the mean ± S.D. for triplicate experiments. PVP (□), 5%-sulfonated PVP (△), 20%-sulfonated PVP (▲), 5%-carboxylated PVP (○), 20%-carboxylated PVP (●), polyacrylic acid (◆), polybrene (■).

polymer. Polybrene was cytotoxic to LLC-MK2 cells and HAEC cells (Fig. 5). In contrast, PVP and anionized PVP derivatives showed very little cytotoxicity. For example, cells treated with 10 mg/ml of anionized PVP derivatives were viable, while lower levels of polybrene (0.1 mg/ml for LLC-MK2 and 1 mg/ml for HAEC) killed more than 50% of the cells. These results indicated that anionized PVPs were extremely safe.

4. Discussion

There is no cure for renal disease, which is a serious problem which is on the increase in the world, and few strategies are available for prevention. To create a renal targeting carrier for renal drug delivery system, this study was conducted to clarify the influence of anionic groups on the pharmacokinetics of polymeric drug carriers. Our results will facilitate the design of renal targeting carriers for therapeutic application. In this study, we used tumor-bearing mice for assessment of in vivo behavior of anionized PVP derivatives, because our research goal is to create polymeric targeting carriers to various tissues, such as kidneys, tumors, and brain. Of course, we have already confirmed that the pharmacokinetics of ^{125}I-labeled polymers were similar in both intact mice as well as mice bearing solid tumors (data not shown). This fundamental approach enabled us to construct a rational strategy for bioconjugation of cytokines and various drugs such as peptides and antineoplastic agents.

Due to the recent advances in structural genomics and pharmacoproteomics, the functions of numerous proteins will be clarified. The therapeutic application of bioactive proteins, such as newly identified proteins and cytokines, has also been highly expected. Since these proteins are generally quite unstable in vivo, their clinical application requires frequent administration at high dosages. This often results in impaired homeostasis in vivo and may cause severe adverse effects. Since cytokines such as TNF-α have diverse actions on various tissues, it is not easy to selectively obtain a favorable function to such proteins (therapeutic effects) among their diverse functions in order to minimize their side effects. To overcome these problems, we attempted to conjugate bioactive proteins with nonionic polymeric carriers such as polyethylene glycol (PEG) [4–7]. The bioconjugation of proteins with PEG increases their molecular size and enhances steric hindrance, both of which are dependent on PEG attached to the protein. This results in the improvement of the plasma half-lives of proteins and stability against proteolytic cleavage, as well as a decrease in its immunogenicity. It was also reported that PEGylation of proteins such as TNF-α, interleukin-6 (IL-6) and immunotoxin could enhance therapeutic potency and could reduce undesirable effects.

The fate and distribution of conjugates between polymeric carriers and drugs can be influenced by its physicochemical properties, such as electric charge and hydrophilic–lipophilic balance [8]. Therefore, to control the in vivo behavior of bioconjugated drugs with polymeric carriers, it is necessary to assess the pharmacokinetic characteristics of the polymeric carriers themselves. We have already assessed the biopharmaceutical properties of various nonionic polymeric drug carriers. As a result, we found that PVP is the most suitable polymeric modifier for prolonging the circulation lifetime of a drug and localizing the conjugated drug in blood. By contrast, polyvinylpyrrolidone-co-dimethyl maleic anhydride [poly(VP-co-DMMAn)], which is one of the anionized PVP derivatives, was found to be a useful candidate as a targeting carrier for a

renal drug delivery system [3]. In this study, to optimize the renal drug delivery system, we assessed the renal targeting capability of anionized PVP derivatives.

The in vivo behavior of anionized PVP derivatives changed by the type and content (molar ratio) of anionic groups. The anionized PVP derivatives in the circulation decreased as the number of anionic groups in the PVP increased (Fig. 1). Anionized PVPs were cleared more quickly from the blood than PVP, and the clearance of carboxylated PVP was similar to sulfonated PVP with the same content of anionic groups. It is well known that endothelial cells and the glomerular capillary wall of the kidneys are coated with highly polyanionic sialoprotein [9]. Therefore, anionic charged polymers, such as anionized dextran, are generally considered to be cleared more slowly from the circulation than nonionic and cationic polymers despite having the same molecular weight [10]. The reason for this discrepancy is not clear, but it is partially due to the difference in the structure of anionized polymers. Polysaccharides, such as dextran, have often been used to characterize pharmacokinetics of polymeric modifiers with various characteristics [11]. Nonionic and cationic polysaccharides were rapidly captured by the RES mainly in the liver after their i.v. injection, but anionized polysaccharides were hardly uptaken to RES because of the electrostatic repulsion between the negative charge of the polymer and the vascular wall [10]. As a result, the plasma half-lives of anionized polysaccharides are longer than those of nonionic and cationic polysaccharides, even if anionized polysaccharides distributed in the kidney. By contrast, PVP did not show any specific tissue distribution (Fig. 2) and mainly remained in blood. Thus, we believed that the anionized PVPs are suitable for assessing the effects of anionic groups on pharmacokinetic characteristics.

Anionized PVPs accumulated in the kidneys, as compared to other tissues such as the liver, spleen and lung 3 h after their i.v. injection (Fig. 2). The renal levels of carboxylated PVPs were about five-fold higher than sulfonated PVPs. Especially, the renal levels of 20%-carboxylated PVP were about 30% of the administered dose. Additionally, carboxylated PVPs did not show any cytotoxicity in vitro (Fig. 4). PAA (100%-carboxylated) and PVP (0%-carboxylated), in contrast, showed little accumulation in the kidney. These results suggest that carboxylated PVPs that contain an optimal content of carboxyl groups might exhibit the highest accumulation in the kidney. On the other hand, sulfonated PVPs showed little accumulation and were mostly detected in the urine at 24 h after administration (Fig. 4). There are few reports on the effects of carboxyl and sulfonic groups in the polymer on the pharmacokinetic characteristics of drug conjugates. We assessed the accumulation sites of anionized PVP derivatives in the kidney by tissue-section analysis, and found that carboxylated PVPs effectively localized and were retained in the renal proximal tubular epithelial cells (Fig. 3). The mechanism of the uptake of carboxylated PVP in the proximal tubular epithelial cells in vivo is currently under investigation.

Several renal drug delivery systems have been previously described. One approach involves pro-drugs that are cleaved by kidney-associated enzymes to release the drugs in the kidney [12]. However, these pro-drugs generally do not accumulate in the kidneys as a result of plasma protein binding and limited transport to the kidney. Low-molecular-weight proteins, such as lysozyme, have been used as carriers because they are reabsorbed by the kidneys [13]. Unfortunately, they also produced strong renal toxicity and cardiovascular side effects. Streptavidin carriers bind to biotin in the kidney, but they are immunogenic and have limited renal accumulation due to their large molecular size [14]. It is important to develop an effective renal drug delivery system that not only targets the kidney but also has excellent safety. Anionized PVP derivatives produced no harmful effects, and the safety of both carboxylated PVP and sulfonated PVP appear to be similar to PEG and PVP which are used clinically (Fig. 5). Thus, anionized PVP derivatives appears to be an extremely safe polymeric carrier with a much higher targeting capacity to the urinary organ. We believe that these carboxylated and sulfonated PVPs may be useful polymeric carriers for drug delivery to the kidney and bladder, respectively.

5. Conclusion

Carboxylated PVPs showed higher renal accumulation than sulfonated PVPs, and about 30% of the administered dose of 20%-carboxylated PVPs was observed in the kidney. Most of 20%-carboxylated PVP accumulated in renal tubules, especially the proximal tubular epithelial cells. This study will provide useful information for the design of novel renal targeting carrier.

Acknowledgements

This study was supported in part by a Grant-in-Aid for Scientific Research from the Ministry of Education, Science and Culture of Japan, and in part by Health Sciences Research Grants for Research on Health Sciences focusing on Drug Innovation from the Japan Health Sciences Foundation (KH63124).

References

[1] Jones CA, McQuillan GM, Kusek JW, Eberhardt MS, Herman WH, Coresh J, Salive M, Jones CP, Agodoa LY. Serum creatinine levels in the US population: third national health and nutrition examination survey. Am J Kidney Dis 1998;32:992–9.

第2特集

ファージ表面提示法を駆使した機能性人工タンパク質の創製とDDSへの応用

向 洋平　堤 康央

はじめに

周知の通り，20世紀後半には数多くの生理活性タンパク質が同定され，種々難治性疾患に対して臨床応用が試みられた．しかし過去の多くの事例が示すように，これら生理活性タンパク質は体内安定性に極めて乏しいために，臨床応用する際には大量頻回投与を余儀なくされ，重篤な副作用を招いてしまっている．さらに，サイトカインなどは一般に，複数種のレセプターを介し，多様な*in vivo*生理活性を有するために，目的とする治療作用以外の作用をも同時に発現してしまう．そのため，生理活性タンパク質の医薬品化は依然として，著しく制限されているのが現状である．一方で近年の疾患プロテオミクス研究などのポストゲノム基礎研究の目覚ましい進展もあいまって，疾病治療に有用なタンパク質が加速度的に同定されてきており，タンパク質療法への期待がますます高まってきている．したがって，疾患プロテオミクス情報などを有効活用したプロテオーム創薬を推進し，有効かつ安全なタンパク質療法を確立していくためには，これらタンパク質固有の問題点を克服できる創薬テクノロジー，すなわちタンパク質療法の最適化をめざしたDDS（Drug Delivery System）の確立が必須となっている．

医薬価値に優れた機能性人工タンパク質の創製

タンパク質療法の最適化に向け，従来から産・官・学の多くのバイオ研究機関が，特定レセプターへの親和性や選択性に優れた“生理活性タンパク質のアミノ酸置換体（機能性人工タンパク質）”を創製するため，Kunkel法などの点突然変異法を用いた構造変異体の作製を精力的に試みている[1,2]．しかし点突然変異法では，まず構造変異体の立体構造や機能をシミュレーションし，トライ・アンド・エラーで生理活性タンパク質の構成アミノ酸を1つずつ別の特定アミノ酸に改変することにより，個々の構造変異体を作製せねばならない．そのうえで目的とする機能性人工タンパク質を同定するために，作製した構造変異体の機能を個別に評価していく必要がある．そのため従来法では，膨大な時間・労力を費やすばかりか，作製しうる構造変異体の多様性（種類）にも限界があるなど，期待

図1　ファージ表面提示法を駆使した機能性人工タンパク質の創製

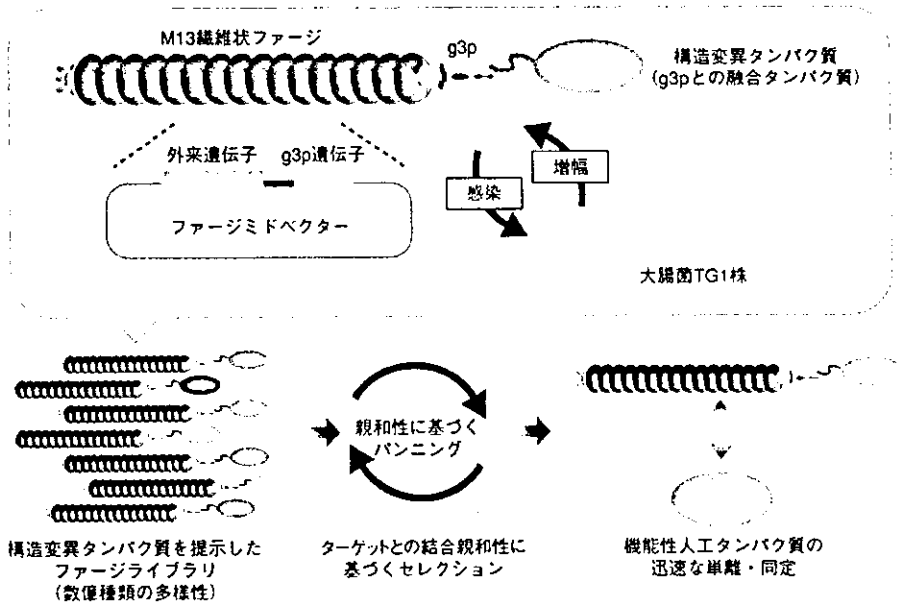

多種多様な構造変異タンパク質を表面提示したファージライブラリ内からの高親和性分子の同定は，パンニングと呼ばれる操作をくり返すことにより行う．パンニングでは，ターゲットの親和性に乏しいクローンを洗浄操作により除き，強固に結合するクローンのみを再度大腸菌に感染させ，増幅する．この操作をくり返すことにより，ターゲットとの高親和性分子を選択・濃縮することが可能である．選択されたクローンに関しては大腸菌に感染させ，コロニーを形成させることにより容易にモノクローン化が可能であり，個々のクローンに関して生物活性，結合親和性の評価やシークエンス解析などの詳細な機能評価を行い，機能性人工タンパク質の同定を行う

図2　高分子バイオコンジュゲーションの特徴

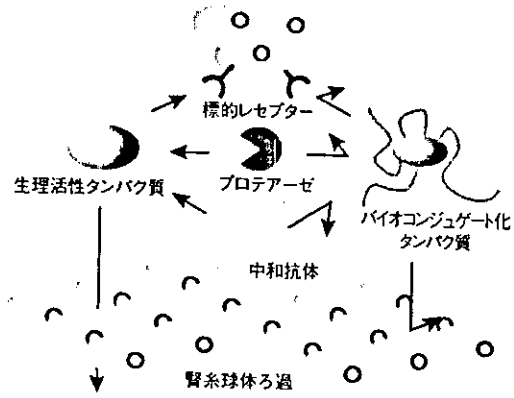

利点
○高分子鎖の形成する立体障害によるプロテアーゼ抵抗性の獲得
○分子量増大に伴う腎糸球体ろ過の回避
○抗原性・免疫原性の低下

問題点
○活性発現に重要な部位への高分子修飾による比活性低下
○高分子鎖の形成する立体障害によるレセプターとの結合阻害

生理活性タンパク質の高分子バイオコンジュゲーションは，上記のような利点を有しており，最終的に生理活性タンパク質の生体内安定性を飛躍的に向上させることが可能である．しかしながらその高分子修飾部位はランダムであり，活性中心への高分子修飾やレセプター結合の阻害に伴う比活性低下という致命的な問題点も有している

通りの成果は得られていない．

一方で近年，バクテリオファージの生活環を巧みに利用し，ターゲット（分子・粒子・細胞）への高親和性結合分子を網羅的かつ迅速に探索・同定しうる基盤技術として，ファージ表面提示法の応用が注目されている[1]．このファージ表面提示法の際だった特徴は，別々の外来性遺伝子産物を表面提示したファージを数億種類以上の多様性に富んだライブラリとして容易に調製可能であり，そのなかからターゲットに対する高親和性に結合するクローンを迅速に単離・同定可能であることなどが挙げられる．また，単離されたクローンに関してはファージに内封される遺伝子の配列から，提示タンパク質のアミノ酸配列を容易に得ることが可能であるといった圧倒的な利点を有している（図1）．しかしながらこのファージ表面提示法は，現在までのところ特定ターゲットに親和性を有する抗体やペプチドを同定する手段として利用されているに過ぎない．そもそもサイトカインなどの生理活性タンパク質をファージ表面に提示させた例すら皆無であった．

われわれは以上の点に着目し，ファージ表面提示法を独自に改良することにより数億種類以上もの多様性を有した構造変異タンパク質（生理活性タンパク質のアミノ酸置換体）を一挙にCombinatorial Biosynthesisし，この構造変異体ライブラリのなかから，レセプター親和性や特異性などが向上した，"医薬価値に優れた機能性人工タンパク質"を迅速かつ効率良く同定できる「プロテオーム創薬のためのタンパク質分子進化戦略」を初めて確立した[1]．

リジン欠損人工TNF-αの創製と部位特異的バイオコンジュゲーション

主として1980年代以降，DDSを視野においた医薬品開発の分野において，生理活性タンパク質の生体内安定性を改善するために，ポリエチレングリコール（PEG）などの水溶性高分子をタンパク質に結合させた，いわゆる高分子バイオコンジュゲーションが考案されてきた[2]．このタンパク質のバイオコンジュゲーションは，分子量増大による腎排泄速度の減少，高分子鎖の形成する立体障害によるプロテアーゼ抵抗性の獲得，抗原性および免疫原性の低下により，最終的にはタンパク質の体内安定性を向上させ，投与量・回数を削減可能となりうる（図2）．しかし，このバイオコンジュゲーションをサイトカインなどへ応用した場合，タンパク質に結合した高分子鎖が形成する立体障害により，レセプターとの結合までもが阻害されてしまい，致命的な比活性低下を引き起こしてしまう．そのため，バイオコンジュゲーションはタンパク質の医薬品化にかなう最適DDSとして位置づけられているものの，その成功例は極度に制限されている．

これまで汎用されてきたバイオコンジュゲーション法は，アミノ基（リジン残基の有するεアミノ基およびN末端のαアミノ基）をターゲットとしたものである．しかしながら，ほとんどのタンパク質においてリジン残基は高次構造の形成やリガンド-レセプター間結合などにも必須の役割を担っている．そのため，これらリジン残基への高分子導入は，必然的に著しい比活性低下を招く結果となっている．また修飾高分子のタンパク質への導入はランダムであるため，得られたバイオコンジュゲート体は，タンパク質のさまざまな部位に種々個数の修飾高分子が結合した，分子的に不均一な混合物となる．その結果，バイオコンジュゲート体は比活性や体内挙動，安定性などの

図3　リジン欠損TNF-αに対する部位特異的バイオコンジュゲーション

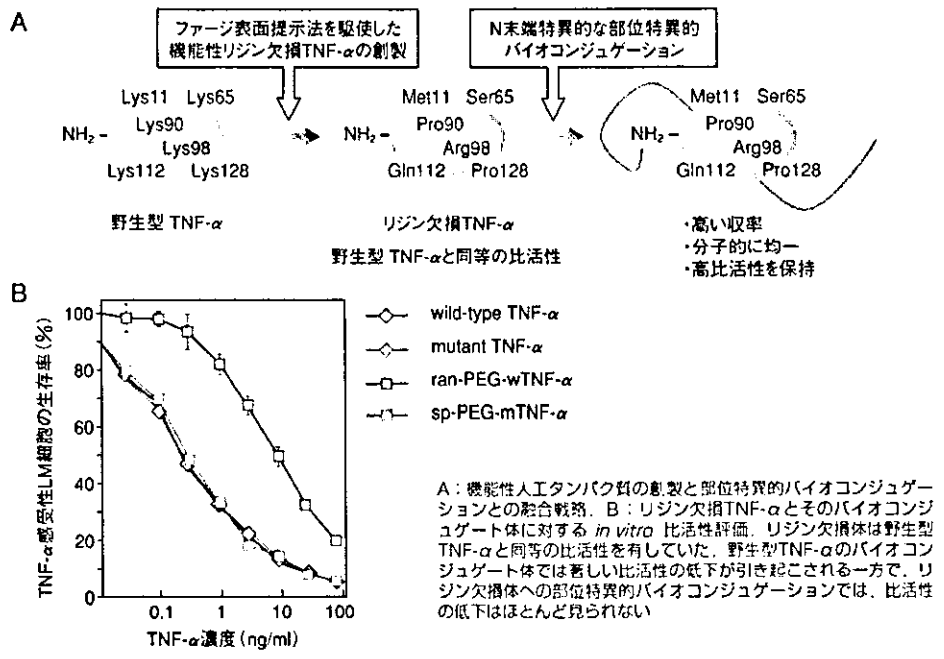

A：機能性人工タンパク質の創製と部位特異的バイオコンジュゲーションとの融合戦略．B：リジン欠損TNF-αとそのバイオコンジュゲート体に対する *in vitro* 比活性評価．リジン欠損体は野生型TNF-αと同等の比活性を有していた．野生型TNF-αのバイオコンジュゲート体では著しい比活性の低下が引き起こされる一方で，リジン欠損体への部位特異的バイオコンジュゲーションでは，比活性の低下はほとんど見られない

機能面でもヘテロな集団となってしまう．しかし現状では，他に適切なタンパク質のDDSが存在しないため，このような問題点を抱えつつも，タンパク質の有効性と安全性確保の観点から，このランダムなバイオコンジュゲーションを医薬開発に適用せざるを得ない．

この点われわれは，前述したファージ表面提示法を駆使した「プロテオーム創薬のためのタンパク質分子進化戦略」により，抗癌剤としての応用が期待される腫瘍壊死因子：TNF αのリジン欠損体を創製することに初めて成功した[1]．このようにタンパク質の活性発現や立体構造維持に必須の役割を担っていると考えられているすべてのリジン残基を欠損させつつも，その生物活性を完全に保持したリジン欠損機能性人工タンパク質を創製し得た例はわれわれを除いて皆無である．TNF-αはN末端が活性発現に重要でないことが過去の報告から明らかとなっており，このリジン欠損TNF-αに対するN末端アミノ基のみを標的とした部位特異的バイオコンジュゲーションは，比活性の低下や分子的不均一性といった従来までのランダム・バイオコンジュゲーションの問題点を一挙に解決可能であると考えた（図3A）．事実，N末端アミノ基への部位特異的モノPEG化リジン欠損TNF-αであるsp-PEG-mTNF-αは80%以上の活性を保持しているなど，圧倒的な利点を有していることが判明した（図3B）．一方で，野生型TNF-αのリジン残基に対し，わずか1分子のPEGが結合したランダムモノPEG化wTNF αであるran-PEG-wTNF-αでは，活性発現や立体構造維持に必須の役割を担っていると考えられているLys11，Lys65，Lys90への高分子導入による比活性低下は避けることができず，その比活性は約10%にまで低下していた．この分子的均一性や比活性，収率に優れた部位特異的PEG化リジン欠損TNF-αは，血中滞留性や抗腫瘍作用の選択的発現能に優れているうえ，従来法で作製したランダムPEG化TNF-αよりも著しく強い*in vivo*抗腫瘍効果を有していることも見出しており，現在臨床応用に向けた研究を推進中である．

この「プロテオーム創薬のためのタンパク質分子進化戦略」を駆使することにより現在までに，レセプター指向性（選択性）や体内安定性に優れた機能性人工TNF-αも多数得ており，TNF-α以外のタンパク質についても，同様の結果を得ている．われわれが確立した分子進化戦略は，"プロテオーム創薬のための競争力"を提供するだけでなく，従来までの点突然変異法（アラニン・スキャン）で得られなかった"タンパク質改変の概念"や"タンパク質の構造-活性相関概念"をも新たに提唱するものである．

おわりに

プロテオーム創薬は，プロテオミクスおよび構造ゲノミクスの進展と，これらの知見を統括したバイオインフォマティクスが駆動力となり，近い将来，上記の分子進化戦略などとの融合により加速度的に推進されるものと期待される．一方でこのようなプロテオーム創薬を指向したバイオインフォマティクスの進展は，タンパク質のアミノ酸配列と立体構造，機能との連関を理解可能とするため，近未来的にはアミノ酸配列が与えられれば，その配列から未知タンパク質の構造と機能が予測し得よう．これは逆に欲する機能と立体構造を有したアミノ酸配列のデザインを可能とするだけでなく，このアミノ酸配列が有する立体構造やその機能を模倣した有機化合物の合理的設計をも可能とする．このようなバイオインフォマティクスをシステムアップするためには，未知タンパク質の機能解明や立体構造解析に加え，種々のタンパク質について膨大な多様性を有する構造変異体を網羅的に作製し，レセプター・リガンド結合の様式，生物活性などをも含めた機能情報を集積し，立体構造との連関を追求しなければならない．この点われわれが開発した分子進化戦略は，視点を変えればわずか1週間で1億種類以上もの多様性を有する構造変異体ライブラリを作製し，その機能情報を高速集積しうる基盤技術といえる．本観点からわれわれは現在，上述の機能性人TNF-αを含むさまざまなタンパク質の構造変異体の機能評価と共に，そのX線結晶構造解析を進めており，近未来的にバイオインフォマティクスへの研究展開を図ろうとしている．

参考文献

1) Tsutsumi, Y. et al.: Proc. Natl. Acad. Sci. USA, 97: 8548-8553, 2000
2) Onda, M. et al.: Cancer Res., 61: 5070-5077, 2001
3) Smith, G. P.: Science, 228: 1315-1317, 1985
4) Yamamoto, Y. et al.: Nature Biotechnol., 21: 546-552, 2003
5) Molineux, G. et al.: Pharmacotherapy, 23: 3S-8S, 2003

堤 康央（つつみやすお）
国立医薬品食品衛生研究所大阪支所医薬基盤研究施設基盤研究第二プロジェクトチーム副プロジェクト長．
1991年大阪大学薬学部薬学科卒業（薬剤学講座，真弓忠範教授），1991年薬剤師免許取得，1993年大阪大学大学院薬学研究科応用薬学専攻修士課程修了（薬剤学講座，真弓忠範教授），1994年大阪大学大学院薬学研究科応用薬学専攻博士課程中退（薬剤学講座，真弓忠範教授），1997年薬学博士（大阪大学）
職歴（研究歴）：1991～1992年国立循環器病センター研究所生体工学部（松田武久部長）外来研究員，1994～1998年大阪大学薬学部助手（薬剤学講座，真弓忠範教授），1998～2004年配置換：大阪大学薬学研究科助手（薬剤学分野，真弓忠範教授），1999～2001年米国National Cancer Institute (NCI) /National Institutes of Health (NIH) 博士研究員（Laboratory of Molecular Biology, Dr. Ira PASTAN），2004年より現職．
受賞：平成16年度　日本薬学会奨励賞，平成16年度　日本薬剤学会奨励賞など
趣味：釣り・テニス・スキューバダイビング
TEL/FAX：072-641-9814（直通），TEL：072-641-9811（内線2320）
FAX：072-641-9812，e-mail：ytsutsumi@nihs.go.jp

Available online at www.sciencedirect.com
SCIENCE DIRECT®
Biochemical and Biophysical Research Communications 317 (2004) 68–76
BBRC
www.elsevier.com/locate/ybbrc

Anti-tumor activity of chemokine is affected by both kinds of tumors and the activation state of the host's immune system: implications for chemokine-based cancer immunotherapy☆

Naoki Okada,[a,*] Jian-Qing Gao,[b,c,*] Akinori Sasaki,[a] Masakazu Niwa,[a] Yuka Okada,[d] Takashi Nakayama,[e] Osamu Yoshie,[e] Hiroyuki Mizuguchi,[f] Takao Hayakawa,[g] Takuya Fujita,[a] Akira Yamamoto,[a] Yasuo Tsutsumi,[b] Tadanori Mayumi,[b] and Shinsaku Nakagawa[b,*]

[a] *Department of Biopharmaceutics, Kyoto Pharmaceutical University, 5 Nakauchi-cho, Misasagi, Yamashina-ku, Kyoto 607-8414, Japan*
[b] *Department of Biopharmaceutics, Graduate School of Pharmaceutical Sciences, Osaka University, 1-6 Yamadaoka, Suita, Osaka 565-0871, Japan*
[c] *Department of Pharmaceutics, School of Pharmaceutical Sciences, Zhejiang University, 353 Yanan Road, Hangzhou, Zhejiang 310031, PR China*
[d] *Department of Pharmaceutics, School of Pharmaceutical Sciences, Mukogawa Women's University, 11-68 Kyuban-cho, Koshien, Nishinomiya, Hyogo 663-8179, Japan*
[e] *Department of Microbiology, Kinki University School of Medicine, Osaka-Sayama, Osaka 589-8511, Japan*
[f] *Division of Cellular and Gene Therapy Products, National Institute of Health Sciences, 1-18-1 Kamiyoga, Setagaya-ku, Tokyo 158-8501, Japan*
[g] *National Institute of Health Sciences, 1-18-1 Kamiyoga, Setagaya-ku, Tokyo 158-8501, Japan*

Received 23 February 2004

Abstract

In this study, we screened the anti-tumor activity of murine chemokines including CCL17, CCL19, CCL20, CCL21, CCL22, CCL27, XCL1, and CX3CL1 by inoculating murine B16BL6, CT26, or OV-HM tumor cells, all of which were transfected with chemokine-expressing fiber-mutant adenovirus vector, into immunocompetent mice. A tumor-suppressive effect was observed in mice inoculated with CCL19/B16BL6 and XCL1/B16BL6, and CCL22/OV-HM showed considerable retardation in tumor growth. In the cured mice inoculated with CCL22/OV-HM, a long-term specific immune protection against parental tumor was developed. However, we were unable to identify the chemokine that had a suppressive activity common to all three tumor models. Furthermore, an experiment using chemokine-transfected B16BL6 cells was also performed on mice sensitized with melanoma-associated antigen. A drastic enhancement of the frequency of complete rejection was observed in mice inoculated with CCL17-, CCL19-, CCL22-, and CCL27-transfected B16BL6. Altogether, our results suggest that the tumor-suppressive activity of chemokine-gene immunotherapy is greatly influenced by the kind of tumor and the activation state of the host's immune system.

Keywords: Adenovirus vector; Chemokine; Transfection; Anti-tumor activity; Gene immunotherapy

Chemokine consists of a superfamily of small (8–14 kDa), secreted basic proteins that regulate relevant leukocyte-migration and -invasion into tissue by interacting with their specific receptors, which belong to the superfamily of seven-transmembrane domain G-protein-coupled receptors [1,2]. The function of chemokine, which is capable of attracting specific immune cells, is demonstrated in inflammatory disease sites as well as normal lymphoid tissues [2]. Because of these properties, chemokine is considered as the intriguing molecule for cancer immunotherapy, which is based on the premise of

☆ *Abbreviations:* Ad, adenovirus vector; AdRGD, RGD fiber-mutant Ad; CTL, cytotoxic T lymphocyte; DC, dendritic cell; FBS, fetal bovine serum; MOI, multiplicity of infection; NK, natural killer; PBS, phosphate-buffered saline; $TCID_{50}$, tissue culture infectious $dose_{50}$.

* Corresponding authors. Fax: +81-75-595-4761 (N. Okada), +81-6-6879-8179 (S. Nakagawa), +86-571-87217376 (J.-Q. Gao).
E-mail addresses: okada@mb.kyoto-phu.ac.jp (N. Okada), gaojq@phs.osaka-u.ac.jp (J.-Q. Gao), nakagawa@phs.osaka-u.ac.jp (S. Nakagawa).

0006-291X/$ - see front matter © 2004 Elsevier Inc. All rights reserved.
doi:10.1016/j.bbrc.2004.03.013

the eradication of tumor cells as a consequence of interaction with immune cells that have migrated and accumulated in tumor tissues [3]. To date, more than 40 chemokines have been identified, and several chemokines have been demonstrated as candidates for cancer treatment for use either as sole agents or with an adjuvant [4–8].

We hypothesized that efficient in vitro transfection of chemokine gene into tumor cells could render the tumor sufficient chemokine expression in vivo for screening anti-tumor activity. The chemokine, secreted from inoculated tumor cells, would induce the accumulation of immune cells in the tumor tissue. Consequently, the interaction between the immune cells and the tumor cells should initiate and/or demonstrate the anti-tumor immune response. Among the various methods of gene transduction, recombinant adenovirus vector (Ad) can provide high-level transduction efficacy to a variety of cell types [9,10]. However, some tumor cells exhibit a resistance to Ad-mediated gene transduction due to a decline in the expression of a coxsackie-adenovirus receptor, a primary Ad-receptor, on their surface. We previously demonstrated that, compared with conventional Ad, the fiber-mutant Ad harboring the RGD sequence in the HI loop of the fiber knob (AdRGD) could more efficiently transduce foreign genes into several kinds of tumor cells due to their directivity to αv-integrin positive in the majority of tumors [11–13]. Therefore, chemokine-expressing AdRGD would be useful not only for screening the anti-tumor activity of chemokines by in vitro transfection, but also for developing in vivo cancer gene immunotherapy.

In the present study, we first confirmed the vector performance of eight AdRGDs encoding each mouse chemokine, CCL17, CCL19, CCL20, CCL21, CCL22, CCL27, XCL1, or CX3CL1. The anti-tumor activity of these chemokines was investigated in mice by inoculating three kinds of murine tumor cells, B16BL6 melanoma, CT26 colon carcinoma, and OV-HM ovarian carcinoma cells, transfected with each chemokine-expressing AdRGD. In addition, we examined the growth and rejection ratio of chemokine gene-transduced B16BL6 cells in mice sensitized with melanoma-associated antigen (gp100).

Materials and methods

Cell lines and animals. Human lung carcinoma A549 cells were purchased from ATCC (Manassas, VA, USA). Murine melanoma B16BL6 cells (H-2^b) and human embryonic kidney 293 cells were obtained from JCRB cell bank (Tokyo, Japan). Murine colon carcinoma CT26 cells (H-2^d) were kindly provided by Dr. Nicholas P. Restifo (National Cancer Institute, Bethesda, MD, USA). Murine ovarian carcinoma OV-HM cells (H-$2^{b/k}$) were kindly provided by Dr. Hiromi Fujiwara (School of Medicine, Osaka University, Osaka, Japan). A549 and 293 cells were maintained in Dulbecco's modified Eagle's medium supplemented with 10% fetal bovine serum (FBS) and antibiotics. B16BL6 cells were cultured in a minimum essential medium supplemented with 7.5% FBS and antibiotics. CT26 and OV-HM cells were grown in an RPMI 1640 medium supplemented with 10% FBS and antibiotics. Murine pre-B lymphoma L1.2 cells and their stable transfectants of a specific chemokine receptor, L1.2/CCR4, L1.2/CCR6, L1.2/CCR7, L1.2/CCR10, L1.2/XCR1, and L1.2/CX3CR1 cells [14], were maintained in an RPMI 1640 medium supplemented with 10% FBS, 50 μM of 2-mercaptoethanol, and antibiotics. All the cell lines were cultured at 37 °C in a humidified atmosphere with 5% CO_2. Female C57BL/6 (H-2^b), BALB/c (H-2^d), and B6C3F1 (H-$2^{b/k}$) mice, ages 7–8 weeks, were purchased from SLC (Hamamatsu, Japan). All of the animal experimental procedures were in accordance with the Osaka University guidelines for the welfare of animals in experimental neoplasia.

Vectors. Replication-deficient AdRGD was based on the adenovirus serotype 5 backbone with deletions of E1/E3 region. The RGD sequence for αv-integrin-targeting was inserted into the HI loop of the fiber knob using a two-step method as previously described [11]. Mouse cDNAs of CCL17, CCL19, CCL20, CCL21, CCL22, and XCL1 were obtained from pExCell-mCCL17, pT7T3D-Pac-mCCL19, pFastBac1-mCCL20, pT7T3D-Pac-mCCL21, pBluescript SK(+)-mCCL22, and pExCell-mXCL1, respectively. The expression cassette containing each mouse chemokine cDNA under the control of the cytomegalovirus promoter was inserted into E1-deletion site for constructing AdRGD-CCL17, -CCL19, -CCL20, -CCL21, -CCL22, and -XCL1, respectively, by an improved in vitro ligation method as previously described [15,16]. Mouse CCL27-expressing AdRGD (AdRGD-CCL27), mouse CX3CL1-expressing AdRGD (AdRGD-CX3CL1), gp100-expressing AdRGD (AdRGD-gp100), β-galactosidase-expressing AdRGD (AdRGD-LacZ), luciferase-expressing AdRGD (AdRGD-Luc), and AdRGD-Null, which is identical to the AdRGD vectors without the gene expression cassette, were previously constructed [11,17–19]. AdRGD-LacZ, -Luc, and -Null were used as negative control vectors in the present study. All recombinant AdRGDs were propagated in 293 cells, purified by two rounds of cesium chloride gradient ultracentrifugation, dialyzed, and stored at −80 °C. Titers (tissue culture infectious $dose_{50}$; $TCID_{50}$) of infective AdRGD particles were evaluated by the end-point dilution method using 293 cells.

RT-PCR analysis. A549 cells were transfected with each AdRGD at an MOI (multiplicity of infection; $TCID_{50}$/cell) of 50 for 2 h, and then the cells were washed twice with phosphate-buffered saline (PBS) and cultured for 24 h. The expression of mouse chemokine mRNA in these A549 cells was confirmed by an RT-PCR analysis as follows: total RNA was isolated from transduced A549 cells using Sepasol-RNA I Super (Nacalai Tesque, Kyoto, Japan) according to the manufacturer's instructions, following which RT proceeded for 60 min at 42 °C in a 50-μl reaction mixture containing 5 μg total RNA treated with DNase I, 10 μl of 5× RT buffer, 5 mM $MgCl_2$, 1 mM dNTP mix, 1 μM random hexamers, 1 μM oligo(dT), and 100 U ReverTra Ace (Toyobo, Osaka, Japan). PCR amplification of each mouse chemokine and human β-actin transcripts was performed in 50 μl of a reaction mixture containing 1 μl of RT-material, 5 μl of 10× PCR buffer, 1.25 U *Taq* DNA polymerase (Toyobo), 1.5 mM $MgCl_2$, 0.2 mM dNTP, and 0.4 μM primers. The sequences of the specific primers used for PCR amplification and the expected PCR product sizes are defined in Table 1. After denaturation for 2 min at 95 °C, 30 (mouse chemokine) or 20 (human β-actin) cycles of denaturation for 30 s at 95 °C, annealing for 30 s at 55 °C (human β-actin), 60 °C (mouse CCL17, CCL19, CCL20, CCL22, and CX3CL1), 62 °C (mouse CCL21 and XCL1), or 63 °C (mouse CCL27), and extension for 30 s at 72 °C were repeated and followed by completion for 4 min at 72 °C. The PCR product was electrophoresed on a 3% agarose gel, stained with ethidium bromide, and visualized under ultraviolet radiation. EZ Load (Bio-Rad, Tokyo, Japan) was used as a 100 bp molecular ruler.

In vitro chemotaxis assay. A549 cells were transfected with each AdRGD at an MOI of 50 for 2 h, and then the cells were washed twice with PBS and cultured in media containing 10% FBS. After 24 h

Table 1
Primer sequences used for PCR amplification

Gene	Primer sequence (5′ → 3′)	Product size (bp)
Mouse CCL17	(F) TGC TTC TGG GGA CTT TTC TG (R) CCT TGG GTT TTT CAC CAA TC	242
Mouse CCL19	(F) GAA AGC CTT CCG CTA CCT TC (R) TGC TGT TGC CTT TGT TCT TG	164
Mouse CCL20	(F) CGA CTG TTG CCT CTC GTA CA (R) CAC CCA GTT CTG CTT TGG AT	157
Mouse CCL21	(F) CTG AGC CTC CTT AGC CTG GT (R) TCC TCT TGA GGG CTG TGT CT	381
Mouse CCL22	(F) TAT GGT GCC AAT GTG GAA GA (R) GCA GGA TTT TGA GGT CCA GA	102
Mouse CCL27	(F) CTC CCG CTG TTA CTG TTG CT (R) AGT TTT GCT GTT GGG GGT TT	331
Mouse XCL1	(F) ATG GGT TGT GGA AGG TGT G (R) GGG AAC AGT TTC AGC CAT GT	250
Mouse CX3CL1	(F) GCA GTG ACC GGA TCA TCT CT (R) GGC ACC AGG ACG TAT GAG TT	701
Human β-actin	(F) CCT TCC TGG GCA TGG AGT CCT G (R) GGA GCA ATG ATC TTG ATC TTC	202

cultivation, cells were washed and incubated with an assay medium (phenol red-free RPMI 1640 containing 0.5% bovine serum albumin and 20 mM Hepes, pH 7.4) for another 24 h. The resulting conditioned medium was collected, and its chemoattractant activity was measured by an in vitro chemotaxis assay across a polycarbonate membrane with 5-μm pores (Chemotaxicell-24; Kurabo, Osaka, Japan) using L1.2 transfectants expressing the specific receptor for chemokines. Recombinant chemokines corresponding to each specific receptor (mouse: CCL19, CCL20, CCL22, CCL27, XCL1, and CX3CL1) were purchased from DakoCytomation (Kyoto, Japan) and used as a positive control for cell migration. Migration was allowed for 2 h at 37 °C in a 5% CO_2 atmosphere. The migrated cells were lysed and quantitated using a PicoGreen dsDNA quantitation reagent (Invitrogen, Tokyo, Japan), and the migration activity was expressed in term of the percentage of the input cells calculated by the following formula: (% of input cells) = (the number of migrated cells)/(the number of cells placed in Chemotaxicell-24; 1×10^6 cells) × 100.

Evaluation of growth of chemokine gene-transduced tumor cells in immunocompetent mice. B16BL6, CT26, and OV-HM cells were transfected with each AdRGD at an MOI of 400, 50, and 10, respectively. After 24 h cultivation, the cells were harvested and washed three times with PBS, and then 2×10^5 transduced B16BL6 cells, 2×10^5 transduced CT26 cells, and 1×10^6 transduced OV-HM cells were intradermally inoculated into the flank of C57BL/6 mice, BALB/c mice, and B6C3F1 mice, respectively. The major and minor axes of the tumor were measured using microcalipers, and the tumor volume was calculated by the following formula: (tumor volume; mm^3) = (major axis; mm) × (minor axis; $mm)^2 \times 0.5236$ [20]. The mice were euthanized when one of the two measurements was greater than 15 mm. On day 60 after tumor inoculation, the tumor-free mice were judged as individuals that could achieve complete rejection. In some cases, the mice that could completely reject a primary tumor were rechallenged by intradermal injection into the flank with 1×10^6 parental or irrelevant tumor cells without chemokine gene-transduction at 3 months after the initial challenge.

Evaluation of growth and rejection ratio of chemokine gene-transduced B16BL6 cells in mice sensitized with melanoma-associated antigen. The immunization of mice with melanoma-associated antigen was performed by the administration of dendritic cells (DCs) transduced with the gp100 gene. The isolation, cultivation, and gene transduction procedures for C57BL/6 mouse bone marrow-derived DCs conformed to the methods previously described [21]. DCs transfected with Ad-RGD-gp100 at an MOI of 50 for 2 h were intradermally injected into the right flank of C57BL/6 mice at 5×10^5 cells/50 μl. At 1 week after the vaccination, 2×10^5 intact or transduced B16BL6 cells were inoculated into the left flank of the mice. The tumor growth and complete rejection were assessed as described above.

Results

Expression of chemokine mRNA and protein in cells transfected with AdRGD

In order to verify the vector performance of mouse chemokine gene-carried AdRGDs, we first examined

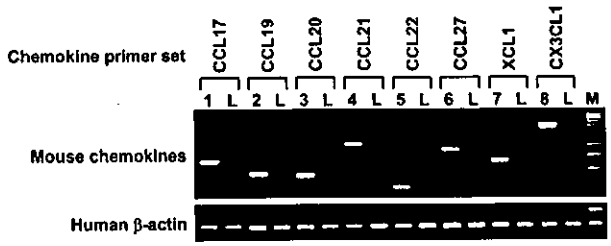

Fig. 1. RT-PCR analysis of chemokine mRNA expression in A549 cells transfected with each chemokine gene-carried AdRGD. PCR for mouse chemokine and human β-actin transcripts was performed on the same RT samples using each specific primer set (summarized in Table 1) to ensure the quality of the procedure. Lane L is negative control using AdRGD-LacZ-transfected A549 (LacZ/A549) cell-derived RT material. Lanes 1–8 represent CCL17/A549, CCL19/A549, CCL20/A549, CCL21/A549, CCL22/A549, CCL27/A549, XCL1/A549, and CX3CL1/A549, respectively. Lane M is a 100 bp molecular ruler.

mRNA expression in transfected cells by an RT-PCR analysis (Fig. 1). In this experiment, human lung carcinoma A549 cells were used instead of murine tumor cells to eliminate the influence of the expression of endogenous mouse chemokine. A549 cells transfected with AdRGD-CCL17, -CCL19, -CCL20, -CCL21, -CCL22, -CCL27, -XCL1, or -CX3CL1 expressed corresponding mouse chemokine mRNA, whereas no PCR products derived from the transcripts of the mouse chemokine gene were detected in AdRGD-LacZ-transfected A549 cells. Next, using in vitro chemotaxis assay, we investigated whether A549 cells transfected with each chemokine gene-carried AdRGD could secrete chemokine protein as a biologically active form into culture supernatants. As shown in Fig. 2, the culture supernatants of each chemokine gene-transduced A549 cell could induce greater migration of cells expressing the corresponding chemokine receptor than those of the intact A549 cells or the AdRGD-Luc-transfected A549 (Luc/A549) cells. The migration of parental L1.2 cells for chemokine receptor-transfectants was not observed in recombinant chemokine-added wells, and they were

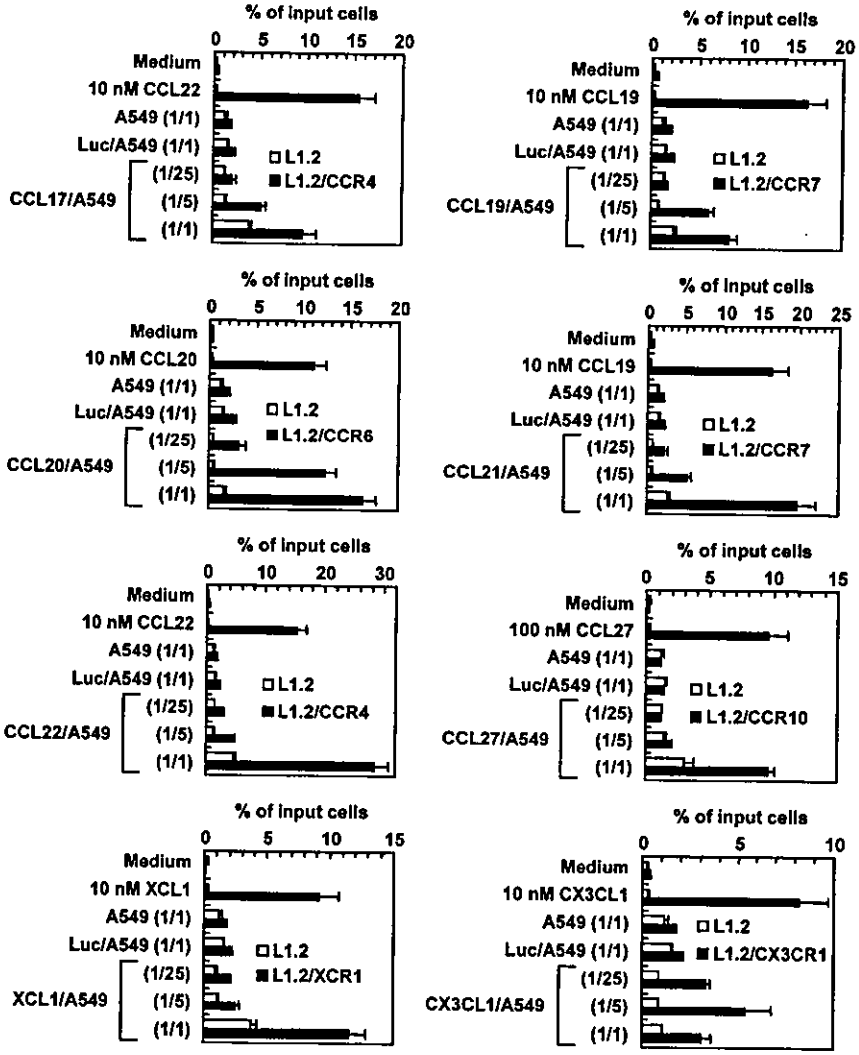

Fig. 2. Chemoattractant activity of culture supernatants of A549 cells transfected with each chemokine gene-carried AdRGD against the stable specific chemokine receptor-expressing cells. The culture supernatants of intact A549 cells, AdRGD-Luc-transfected A549 (Luc/A549) cells, and chemokine gene-transduced A549 cells were prepared and diluted with an assay medium. The fractional values with parentheses in each panel express the dilution factor. These samples and recombinant chemokines dissolved with the assay medium were added to a 24-well culture plate. Cells expressing specific receptors for CCL17 and CCL22 (L1.2/CCR4), CCL20 (L1.2/CCR6), CCL19 and CCL21 (L1.2/CCR7), CCL27 (L1.2/CCR10), XCL1 (L1.2/XCR1), or CX3CL1 (L1.2/CX3CR1) were suspended with the assay medium and placed in a Chemotaxicell-24 installed on each well at 1×10^6 cells. Likewise, parental L1.2 cells for these transfectants were prepared and added to Chemotaxicell-24. Cell migration was allowed for 2 h at 37 °C in a 5% CO_2 atmosphere. The cells that migrated to the lower well were lysed and quantitated using a PicoGreen dsDNA quantitation reagent. The data are expressed as means ± SE of the triplicate results.

maintained at low levels against the culture supernatants of intact A549, Luc/A549, and chemokine gene-transduced A549 cells. These results clearly demonstrated that all AdRGDs encoding each chemokine gene could deliver the concerned gene to target cells, and that transfected cells could secrete the chemokine protein which maintained original chemoattractant activity.

In vivo anti-tumor effect by transfection with chemokine-expressing AdRGD

B16BL6 and CT26 cells were each transfected with eight kinds of chemokine-expressing AdRGDs and AdRGD-Luc, as a control vector, at an MOI of 400 and 50, respectively. OV-HM cells were transfected with

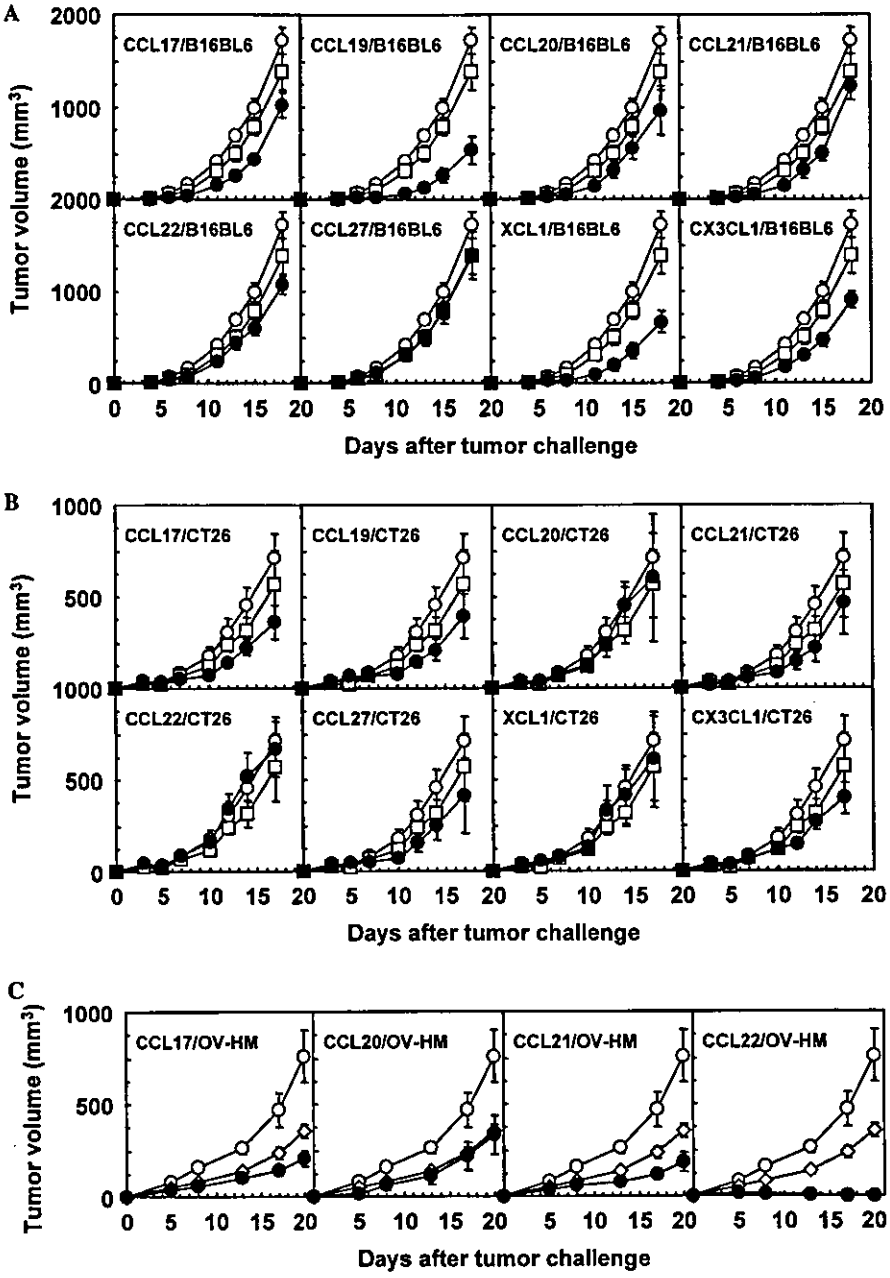

Fig. 3. In vivo growth of three kinds of murine tumor cells transduced with the chemokine gene. B16BL6 cells (A), CT26 cells (B), and OV-HM cells (C) were transfected with each chemokine-expressing AdRGD at an MOI of 400, 50, and 10, respectively, for 24 h. C57BL/6 mice, BALB/c mice, and B6C3F1 mice were intradermally injected in the flank with 2×10^5 transduced B16BL6 cells, 2×10^5 transduced CT26 cells, and 1×10^6 transduced OV-HM cells (●), respectively. Similarly, mice were inoculated with three kinds of intact tumor cells (○), AdRGD-Luc-transfected B16BL6 cells or CT26 cells (□), or AdRGD-Null-transfected OV-HM cells (◇), as control groups. The tumor volume was calculated after measuring the major and minor axes of the tumor at indicated points. Each point represents the mean ± SE of 6–10 mice. The data are representative of two independent experiments.

AdRGD-CCL17, -CCL20, -CCL21, -CCL22, or control AdRGD-Null at an MOI of 10. These transduced tumor cells were intradermally inoculated into H-2 haplotype-matched mice, and tumor growth was compared with that of intact tumors. As shown in Fig. 3, the tumorigenicity of B16BL6 and CT26 cells was hardly affected by transfection with the control vector, whereas OV-HM cells transfected with AdRGD-Null exhibited a slight delay of tumor growth as compared with intact OV-HM cells. Among 20 combinations of chemokine and tumor cells, an obvious tumor-suppressive effect was recognized in mice inoculated with CCL19/B16BL6, XCL1/B16BL6, or CCL22/OV-HM cells. In contrast, the in vivo growth of CCL27/B16BL6, CCL20/CT26, CCL22/CT26, XCL1/CT26, and CCL20/OV-HM cells was the same as that of the control vector-transfected cells, and only a slight delay of tumor growth was observed in five B16BL6 groups (CCL17, CCL20, CCL21, CCL22, and CX3CL1), five CT26 groups (CCL17, CCL19, CCL21, CCL27, and CX3CL1), and two OV-HM groups (CCL17 and CCL21). Importantly, CCL22/OV-HM cells not only demonstrated considerable retardation in tumor growth but were also completely rejected in 9 of 10 mice. In the rechallenge experiment, these cured mice were intradermally injected with 1×10^6 parental OV-HM cells or irrelevant B16BL6 cells at 3 months after the initial challenge. Five of six mice rechallenged with OV-HM cells remained tumor-free for more than 2 months, whereas rechallenging with B16BL6 cells perfectly developed palpable tumors in three additional mice within 2 weeks (data not shown). These results indicate the generation of long-term specific immunity against OV-HM tumor in mice that could once reject CCL22/OV-HM cells.

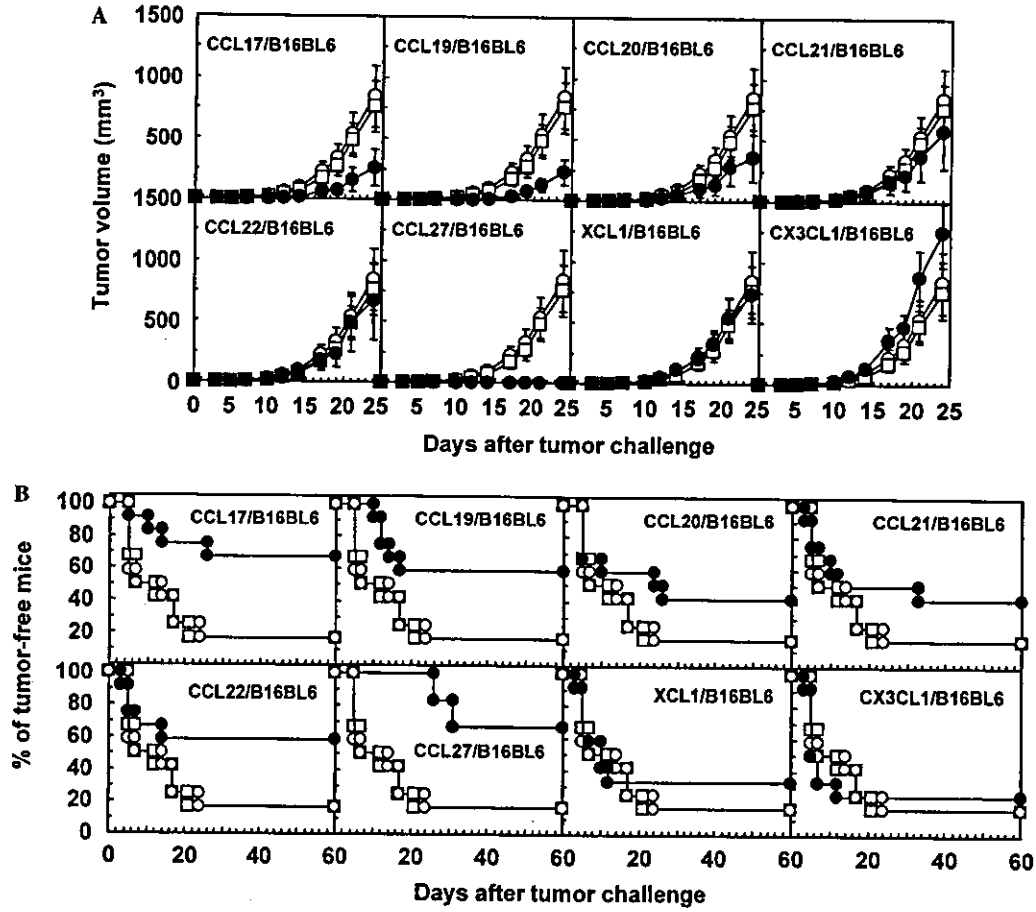

Fig. 4. Growth and rejection ratio of B16BL6 cells transduced with the chemokine gene in mice primed with melanoma-associated antigen. C57BL/6 mouse bone marrow-derived DCs were transfected with AdRGD-gp100 at an MOI of 50 for 2 h and they were intradermally injected into the right flank of syngeneic mice at 5×10^5 cells. At 1 week after the vaccination, these mice were intradermally inoculated in the left flank with 2×10^5 B16BL6 cells transfected with each chemokine-expressing AdRGD at an MOI of 400 for 24 h (●). Likewise, intact B16BL6 cells (○) or AdRGD-Luc-transfected B16BL6 cells (□) were inoculated in the gp100-primed mice, which were used as control groups. (A) The tumor volume was assessed three times per week. Each point represents the mean ± SE of results obtained from 12 mice. (B) Data are expressed in terms of the percentage of mice without visible tumor against the total mice tested in each group.